Section 4. Physico-Chemical Biology

https://doi.org/10.29013/ELBLS-23-1-32-41

Son Nguyen Ngoc,
Huong Nguyen Thi,
Institute chemistry and materials
17 Hoang Sam, Nghia Do, Cau Giay, Ha Noi, 100000, Viet Nam

CHARACTERIZATION AND ANTIBACTERIAL ACTIVITIES OF ZNO NANOPARTICLES SYNTHESIZED FROM GUAVA LEAF EXTRACTION

Abstract. In recent years, the method of synthesizing materials with limited use of chemicals has attracted the attention of many researchers. Zinc oxide particles, an object with potential in biomedical applications, has also been synthesized by this method. In this study, ZnO NPs were prepared by a very simple green synthesis method using zinc acetate hexahydrate and using guava leaf extract which acted as capping agents without using any additional chemicals. any. Zinc oxide nanoparticles synthesized by this pathway (GL-ZnO) have been described by X-ray, EDX, FTIR, and SEM techniques. The results show that GL-ZnO has high purity, uniform size, and fineness at the nanoscale. The influence of synthesis conditions on the characteristics of ZnO NPs was evaluated. The IR, and EDX results demonstrate the formation of ZnO NPs, while the SEM results show the size of ZnO at the nanoscale. ZnO NPs showed good antibacterial activity against several gram-negative and gram-positive strains such as E. coli, B. subtilis, and S. cerevisiae.

Keywords: ZnO nanoparticles, Guava leaves, antibacterial.

1. Introduction

Zinc oxide nanoparticles (ZnO NPs) are one of the metal oxides attractive to many researchers for their unique properties and applications. It is cheap, abundant, safe, and easy to prepare. ZnO has a broad energy band (3.37 eV) and a high binding energy of 60 meV, whereby they are thermally, electrically, and chemically stable. ZnO NPs also have low toxicity, increased UV radiation absorption, and strong antibacterial properties. As a result, ZnO NPs are widely studied in applications such as biomarkers, biosensors, drug delivery agents, gene delivery, and nanopharmaceuticals. ZnO is also certified by the US Food and Drug Administration (FDA) as a "GRAS" (generally recognized as safe) substance.

Regarding biology, ZnO NPs have high biocompatibility and antibacterial and antifungal properties [1; 2]. Pham et al [3] synthesized ZnO NPs from orange peel extract and evaluated their antibacterial activity. The reaction conditions including pH, and annealing temperature were investigated to give the optimal synthesis conditions. The synthesized nanoparticle has a size of 30 nm, high antibacteri-

al activity, over 99.9% against E. coli, and 89–98% against S. aureus despite the absence of UV light.

G. Madhumitha et al. [4] used phytochemicals present in Pithecellobium dulce bark extract as stabilizing agents to synthesize ZnO NPs. Nanoparticles have been evaluated for their photo degradability with some water contaminants in the fiber industry such as methylene blue (MB). Antifungal activity against some species such as Aspergillus flavus and Aspergillus niger has been evaluated with relatively high results. At 500 ppm and 1.000 ppm, the antibacterial activity against these fungi was 37.81%, 63.57%, and 40.21%, 43.04%, respectively.

In another remarkable publication by Satarudra P. S. et al [5], quantum dot zinc oxide particles were synthesized using Eclipta alba leaf extract as a reducing agent. The optimal synthesis conditions were confirmed to be at pH 7.5 mL of zinc acetate solution (5 mM) together with 7 mL of the reaction extract for 75 min. TEM results confirmed that there are ZnO particles about 5 nm in size in the post-reaction solution. Selective electron scattering (SAED) analysis recorded the crystalline nature of ZnO having a hexagonal wurtzite phase with lattice constants a = b = 0.32 nm and c = 0.52 nm. The bioactivity evaluation results showed that the antibacterial ability of ZnO was significantly enhanced with the size achieved by the nanoparticles.

Research group of Sanaz A. [6] synthesized and evaluated the photodegradation activity and antibacterial activity of ZnO NPs from the leaf extract of Sambucus ebulus. The crystal phase size of the obtained nanoparticles is about 17 nm. The efficiency of photodegradation with MB pollutants was about 80% after 200 minutes of treatment. The ZnO nanoparticles synthesized by this method showed significant antibacterial efficacy compared to other commercial or crude forms of ZnO and they increased with the processing time.

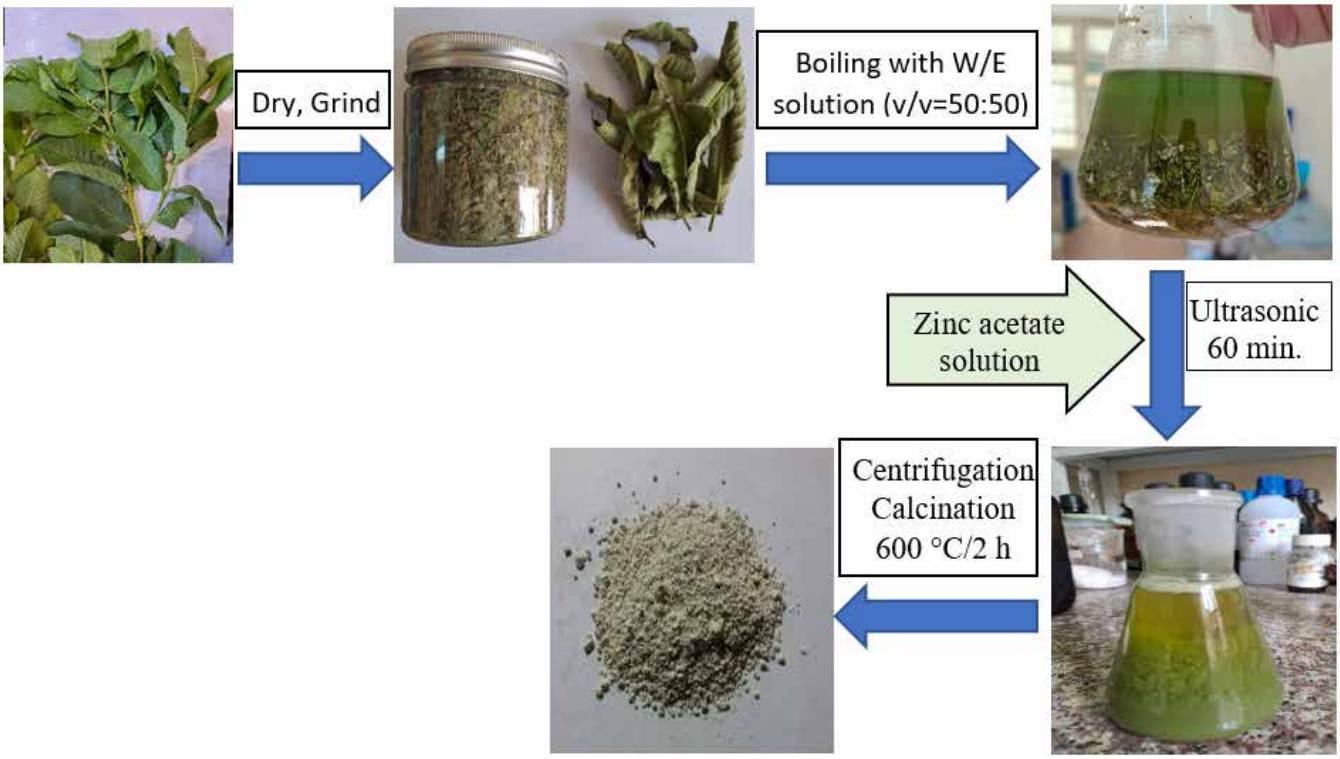

Figure 1. Schematic diagram of ZnO NPs synthesis from guava leaf extract (GL-ZnO)

ZnO NPs are synthesized by chemical, physical, or even biological methods. Precipitation [7; 8], microemulsion [9], sol-gel [10; 11], solvothermal [12; 13], or hydrothermal [14; 15] are examples of chemical processes that consume so much energy or require high temperature and pressure. In the current trend, methods use few or no auxiliary chemicals to synthesize materials to minimize environmental and human impact and reduce costs. Among these, the green synthesis method using plant extracts attracted the most research. ZnO is also the object of many syntheses of this method in orientation for biomedical applications.

Guava is grown in tropical and subtropical countries. In Vietnam, guava leaves are considered a remedy for treating many diseases, such as dysentery, controlling diabetes, losing weight, reducing bad cholesterol, and curing skin allergies. Previous studies have identified guava leaves are rich in phenolic compounds, flavonoids, triterpenoids, tannins, vitamins, essential oils, and sesquiterpene alcohols [16; 17]. As a result, they are the object of attraction for many researchers. Sampath Kumar NS. Et al. [18] took advantage of guava leaf extract's antioxidant and antibacterial activity (GJ) to make jelly without synthetic additives. The results showed that agar from guava leaf extract had high nutritional content with 45.78 g/100 g carbohydrate, 3.0 g/100 g protein, 6.15 mg/100 g vitamin C, 2.90 mg/100 g vitamin B3, and energy 120.6 kcal. The antibacterial activity of guava leaf agar also varied from 11.4 to 13.6 mm against different bacteria. The antioxidant action of GJ towards DPPH free radical was 42.38% and 33.45% for hydroxyl radical. Mass spectrometry confirmed the extract's presence of esculin, quercetin, gallocatechin, 3-sinapoylquinic acid, gallic acid, citric acid, and ellagic acid. These are thought to be the components that contribute to the antibacterial and antioxidant properties of guava leaf extract. In another interesting study, B. Biswas et al. [19] tested the antibacterial activity of guava leaf extract in 4 solvents with increasing polarity, namely hexane, methanol, ethanol, and water, against strains – gram-negative and gram-positive bacteria. The results showed that guava leaf extract using methanol and ethanol solvents had a higher antibacterial effect. Specifically, for the methanol extract, the diameter of the inhibition zone was 8.27 mm and 12.3 mm, and the ethanol extract was 6.11 mm and 11.0 mm, respectively, for B. cereus and S. aureus strains, respectively. These results suggest the potential of guava leaf extract to be used as a natural antibacterial agent.

In this study, we present a green method to synthesize ZnO NPs by using the extraction of guava leaf without adding auxiliary chemicals. The antibacterial activity of the synthesized ZnO NPs was also tested against gram-negative and gram-positive strains including *E. coli*, *B. subtilis,* and *S. cerevisiae*.

2. Materials and methods

2.1. Materials

Guava leaves are harvested at the farm (geographic coordinates: 21.037461, 105.719186) in the summer. Zinc acetate dihydrate ($Zn(CH_3COO)_2 \cdot 2H_2O$) (Merck) as the zinc source; double distilled water and ethanol (Sigma-Aldrich) as the solvents.

2.2. Preparation of Guava leaves extracts

Guava leaves are washed and dried at 32–35°C, 50–57% RH for 2–3 days. Guava leaves were ground and boiled with a mixture of twice distilled water/ethanol (v/v = 50 : 50) at 60 °C for 90 minutes. The guava leaf residue was filtered out; the solution was centrifuged at 5000 rpm for 10 minutes to remove the suspended residue completely. The obtained guava leaf extract was stored at 3–5 degrees Celsius for the following synthesis steps.

2.3 Synthesis of ZnO nanoparticles

50 mL of guava leaf extract was diluted with 50 mL of distilled water. The entire solution was loaded into a single-necked flask in the ultrasonic bath. Dissolve 2 g of zinc acetate in 20 mL of double distilled water. ZnO NPs were synthesized by dripping zinc acetate into guava leaf extract solution,

combined with ultrasound for 60 minutes. The reaction mixture was centrifuged at 10.000 rpm for 5 minutes; the solids were dried at 50 °C for 1 hour before calcining at 600 °C for 2 hours to obtain ZnO NPs. The synthesis process of ZnO NPs is depicted in (Fig. 1).

2.4. Characterization of ZnO NPs

X-ray scattering spectroscopy was used to characterize the crystalline properties of GL-ZnO. The crystal size was calculated using the Scherrer equation (1). The bonds in the synthesized nanoparticle product were studied by FTIR spectroscopy. Their chemical composition was checked by EDX spectroscopy.

$$D = \frac{K \cdot \lambda}{\beta cos\theta} \quad (1)$$

where:

- D is the mean size of the ordered (crystalline) domains, nm;
- K is a dimensionless **shape factor**, with a value close to unity. The shape factor has a typical value of about 0.9;
- λ is the X-ray wavelength, nm;
- β is the line broadening at half the maximum intensity (FWHM), radian;
- θ is the Bragg angle, radian.

2.5. Antibacterial activity test

Antibacterial activity of ZnO was evaluated against gram-positive (*Saccharomyces cerevisiae, Bacillus subtilis* (ATCC9/58) and gram-negative (*E. coli* ATCC 25922) bacteria using the Agar well diffusion method [20]. For microbiological cultivation, the enrichment medium containing meat extract, yeast extract, peptone, glucose, and some mineral salts was utilized. To prepare nutrient agar plates, 37.0 grams of nutrient agar powder was dissolved in 1000 mL of distilled water, and then sterilized in an autoclave at 121 °C /15 lbs pressure for 20 min.

After sterilization treatment, the nutrient agar medium was put into sterile Petri dishes and allowed to solidify. Next, mature broth culture of specific pathogenic bacterial strains in the nutrient broth while distributing all over the surface of agar plates using sterilized L-shaped glass rod. Chitosan and positive-negative control discs were taken into the test for comparison.

The antibacterial activity experiments were conducted with synthesized ZnO NPs and dissolved in 1 mL of DMSO 10% to obtain 200 µg/mL solutions. Under aseptic conditions, 5±1 mm diameter wells were drilled in each Petri dish using the sterile steel cork. Then, 100 µL ZnO NPs were dispersed in 10% DMSO solution and controlled by standard antibiotic Ampicillin (1 mg/ml) as a positive control into the wells. The plates were incubated at 37 °C for 24h before using geometrical Vernier calipers in mm to observe the Zone of inhibition around the wells.

3. Results and Discussion

3.1. Effect of annealing temperature

The experimental process shows that the calcination temperature strongly affects the GL-ZnO product. The heating temperatures from 400 °C, 600 °C, and 800 °C were tested, the effects were observed by scanning electron microscope (SEM) images, and the chemical composition was determined by EDX spectroscopy. The results are shown as shown in the figure… shows that with the temperature of 400 °C, the nanoparticle size is quite large, the uniformity is low, and the ratio of O/Zn atoms is approximately 63/37. This shows that the product has not been completely pyrolysis at this temperature, possibly because the organic part has not decomposed completely. With higher temperatures, it is possible to see the nanoparticles with smaller size, fineness, and a higher degree of uniformity. Along with that is the asymptotic O/ZnO ratio of 50/50. At the calcination temperature of 800 °C, the nanoparticle size is 25–30 nm, and the ratio of O/Zn atoms is 51.2/48.8, showing that almost the product after calcination has only ZnO. Thus, this temperature was chosen to synthesize GL-ZnO for further studies.

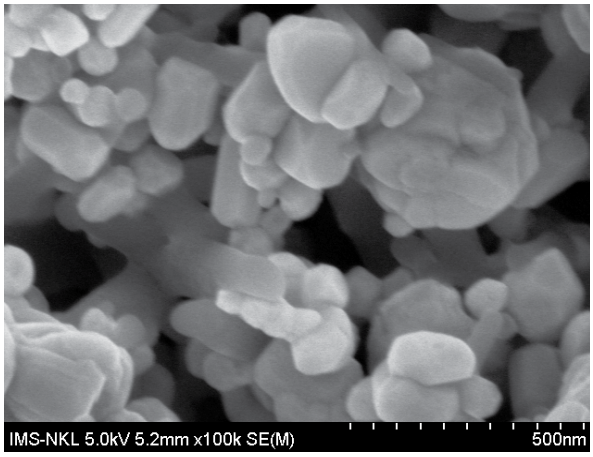

400°C

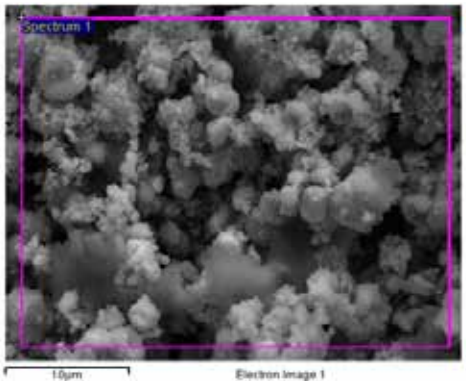

Elements	Weight%	Atomic%
OK	29.01	62.54
ZnK	70.99	37.46
Total	100.00	

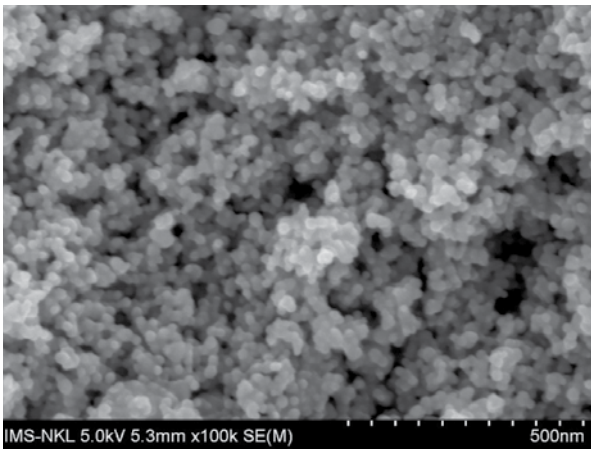

600°C

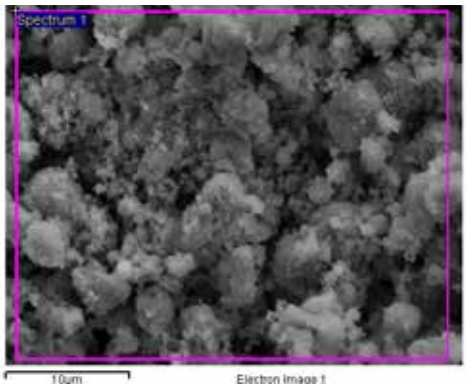

Elements	Weight%	Atomic%
OK	21.94	53.45
ZnK	78.06	46.55
Total	100.00	

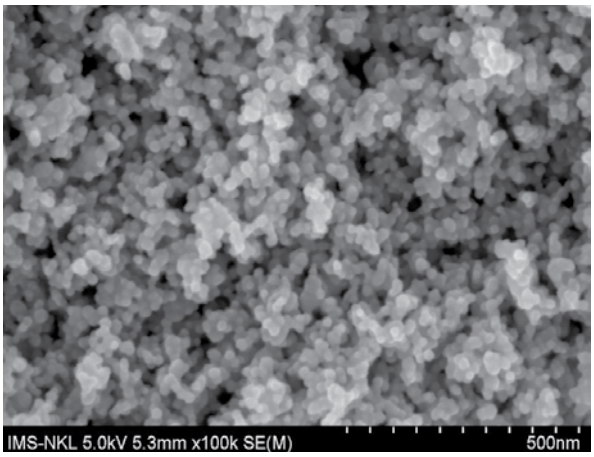

800°C

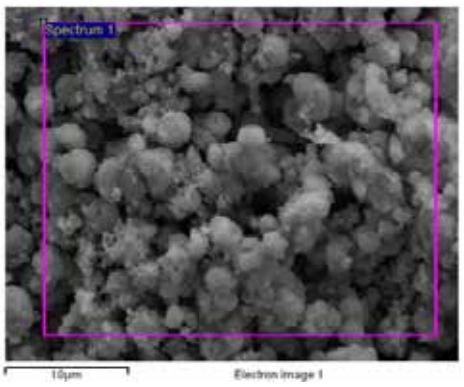

Elements	Weight%	Atomic%
OK	20.43	51.20
Zn K	79.57	48.80
Total	100.00	

Figure 2. SEM (left) and EDX (right) results of GL-ZnO at different calcining temperatures

3.2 Characterization of- ZnO

The XRD pattern of the as-prepared ZnO NPs (Figure 3) showed peaks scattering angle 2 thetas at 31.79°, 34.44°, 36.28°, 47.56°, 56.59°, 62.88°, 66.39°, 67.96°, 69.15°, corresponding to (100), (002), (101), (102), (110), (103), (200), (112), (201) lattice planes.

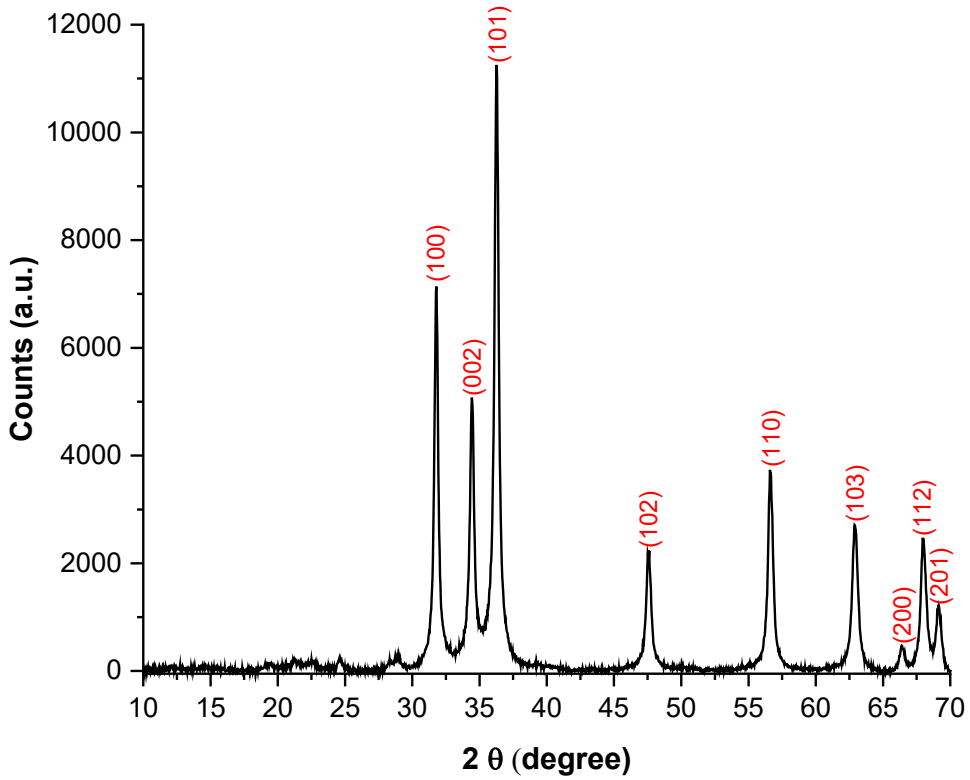

Figure 3. XRD pattern of GL-ZnO

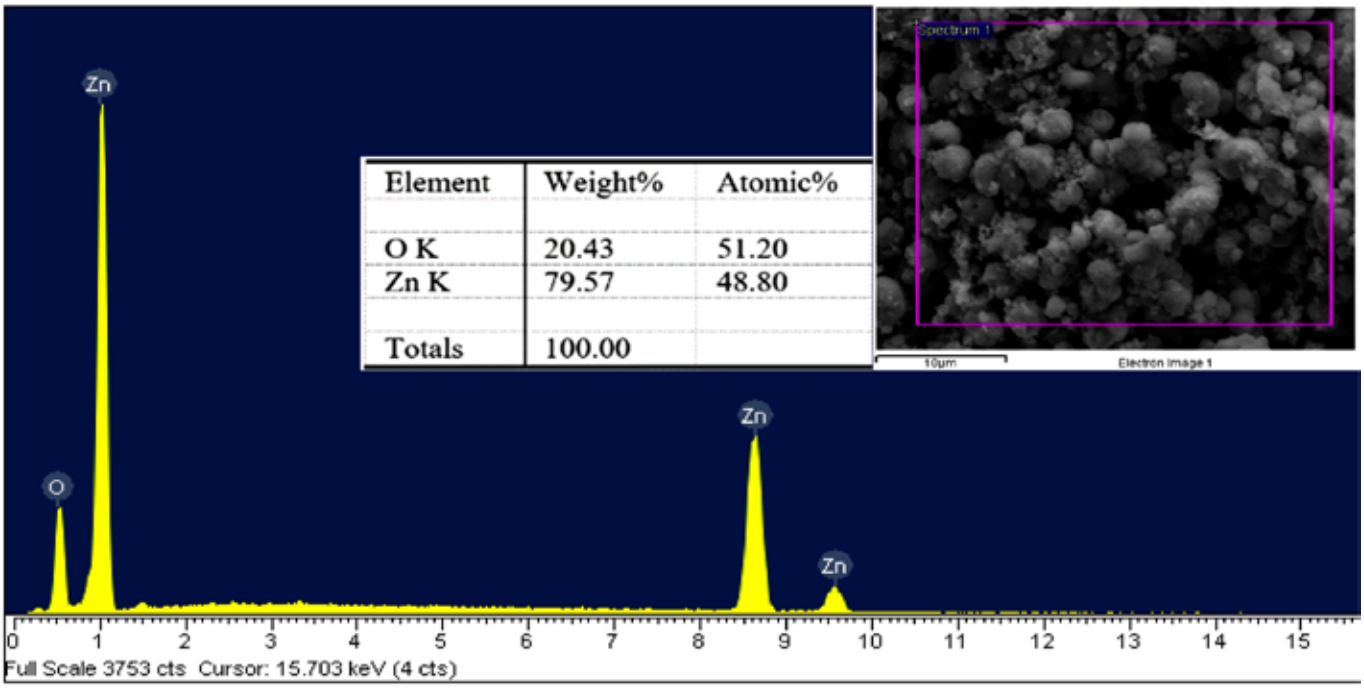

Figure 4. EDX spectrum of GL-ZnO

This result is entirely fitted with the standard XRD pattern of ZnO NPs (JCPDS:36–1451). In addition, the XRD pattern with sharp, intensity peaks, and almost no peaks other than those of ZnO NPs proves that the prepared nanoparticles have a well-crystallized structure and high purity. The EDX results (Figure 4) show only two elements, oxygen, and zinc, with approximately equal atomic ratios. This agrees with the theory and further confirms the purity of the ZnO NPs synthesized by this work. The crystallite size of the nanoparticles calculated by the Scherrer equation is more than 18 nm. As mentioned above, the atomic ratio of these two elements, reaching 51.2/48.8, is approxi-mately the ideal ratio of 1/1. This result shows that the purity level of the GL-ZnO product is very high.

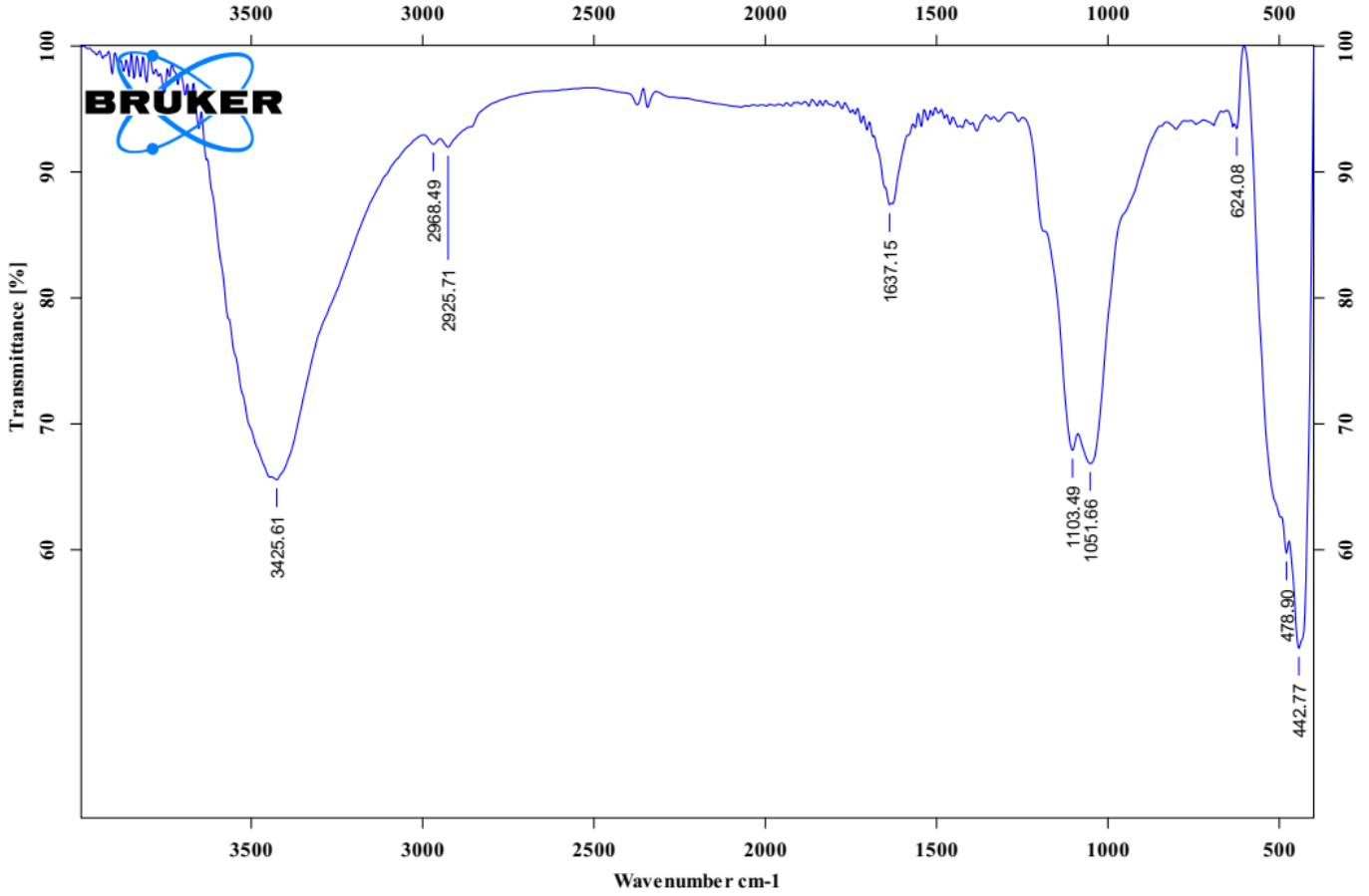

Figure 5. FTIR spectrum of GL-ZnO

The band around 450 cm^{-1} is assigned to the tensile vibration of the Zn-O bond. In addition, in the spectrum, there are signs of the presence of phenolic compounds in the GL extract with strong absorption peaks at wave numbers 3425 cm^{-1} assigned to the valence vibration of the O-H bond, 1051 cm^{-1} and 1103 cm^{-1} represent the valence vibrations of the C-O bond and 1640 cm^{-1} represent the valence band of the C=C and C=O bonds. The weaker absorption band in the region 2925–2968 cm^{-1} is also observed showing the presence of CH_2, and CH_3 groups. In the FTIR spectrum of ZnO, peaks are also observed at this position. It is probably because the calcination time of ZnO is not long enough, and the organic components that act as the capping agent have not been completely pyrolysis.

3.3 Antibacterial activity of GL-ZnO

Figure 6 (a, b, c) depicts testing materials sprinkled on Petri dishes infected with testing microorganisms. The results suggested that ZnO NPs achieved the high-

est capability to inhibit *Bacillus subtilis*. Additionally, clear zones (non-bacterial zones) formed at the sites where ZnO NPs were sprinkled over *Bacillus subtilis*-inoculated Petri dishes.

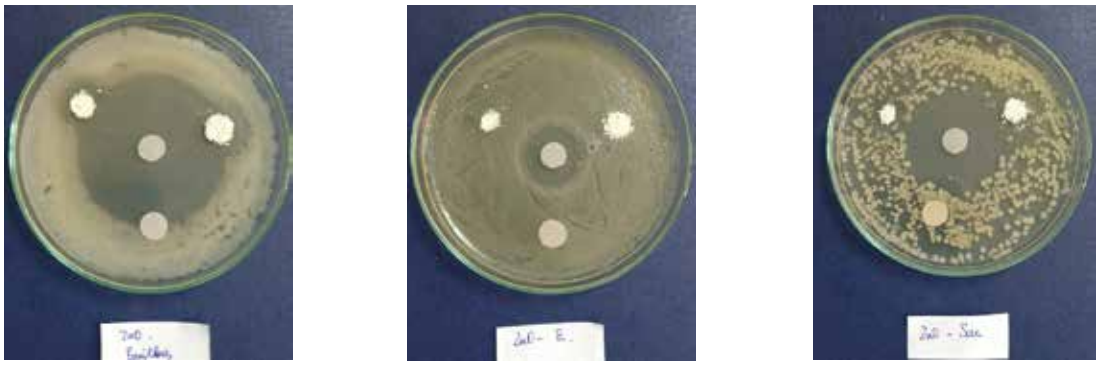

a b c

Figure 6. Antibacterial activities of ZnO NPs against bacterial Control samples: Bacillus (a), E.coli (b), S.cerevisiae (c)

Table 1.– Antibacterial activity of ZnO NPs on selected bacterial strains

Samples	**Concentration**	**Zone of inhibition in mm**		
		E. coli **(Mean±SE)**	***Bacillus*** **(Mean±SE)**	***Saccharomyces*** **(Mean±SE)**
ZnO NPs	15 mg	–	6 ± 0.14	2 ± 0.15
ZnO NPs	30 mg	–	7 ± 0.17	4 ± 0.16

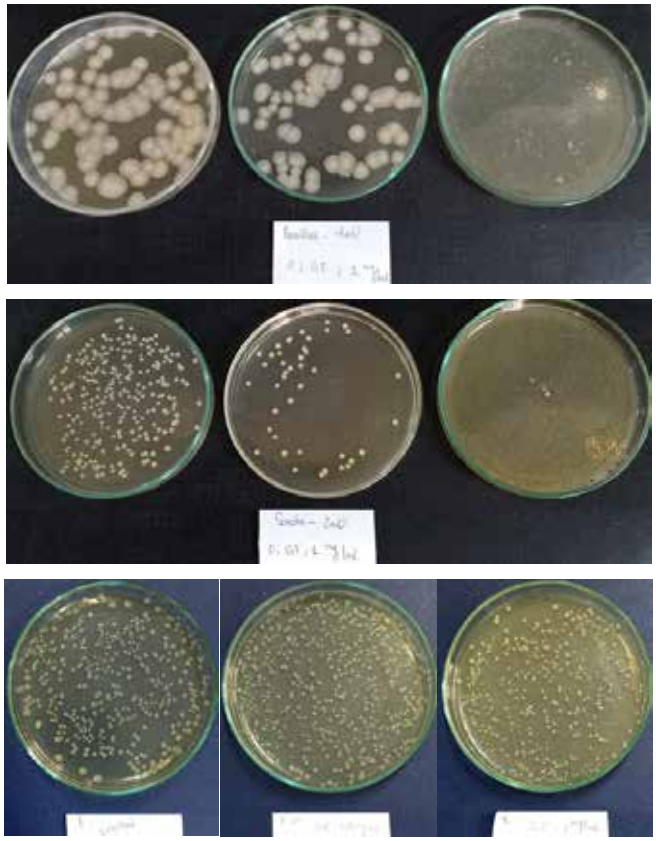

Figure 7. Images showing the antibacterial activities of ZnO NPs with different concentrations

The testing of the capacity of materials to inhibit large microorganisms when exposed to suspensions of the testing organisms as illustrated in Figure 7. Without the requirement for testing materials, the suspensions were evenly dispersed on the controlled plates, and the proliferation of microorganisms on the dish surfaces was also observed. Yet, when *Bacillus subtilis* and *S.cerevisiae* samples solution was exposed to ZnO NPs, the cellular density decreased significantly. Hence, ZnO NPs were able to suppress *Bacillus subtilis* and *S.cerevisiae.*

Figure 7 shows images of the Petri dishes, which is the MIC test results of the ZnONPs. The MIC values against *E. coli, B. subtilis, S. cerevisiae* of ZnONPs were 1.0, 0.5, and 0.5 mg/ml, respectively.

ZnO nanoparticles interact with the membrane of bacterial cells and bind to the mesosome. This mesosome's DNA replication, cell division, and cellular respiration capabilities were diverted, resulting in a larger bacterial cell membrane surface area. On the surface of ZnO NPs, the heavy metal ions Zn^{2+} interact with the microbial cell membranes. The nanoparticles then react quickly with the harmful bacteria to destroy their membrane integrity and cells, resulting in the death of the pathogens [21; 22].

4. Conclusion

This study proposed a straightforward method to synthesize ZnO NPs with almost no use of alkalis as the precipitating agent. The XRD and EDX results have verified that the synthesized ZnO NPs are smaller than 30 nm and high purity. Antibacterial tests with strains of gram-negative bacteria (Bacillus), and fungi (Saccharomyces) show that as-prepared ZnO NPs have a reasonably good killing effect on bacteria with minimum inhibitory concentrations (MIC) are 1.0, 0.5 and 0.5 mg/ml, respectively.

References:

1. Ilves M., et al. Topically applied ZnO nanoparticles suppress allergen induced skin inflammation but induce vigorous IgE production in the atopic dermatitis mouse model. Part Fibre Toxicol,– 11. 2014.– 38 p.
2. Lembo G., et al., Zinc oxide: A new formulation specifically for sensitive skin. Annali Italiani di Dermatologia Allergologica Clinica e Sperimentale,– 60. 2006.– P. 68–72.
3. Thi T. U.D., et al., Green synthesis of ZnO nanoparticles using orange fruit peel extract for antibacterial activities. RSC Advances,– 10(40). 2020.– P. 23899–23907.
4. Madhumitha G., et al., Green synthesis, characterization and antifungal and photocatalytic activity of Pithecellobium dulce peel-mediated ZnO nanoparticles. Journal of Physics and Chemistry of Solids,– 127. 2019.– P. 43–51.
5. Singh A. K., et al., Green synthesis, characterization and antimicrobial activity of zinc oxide quantum dots using Eclipta alba. Materials Chemistry and Physics,– 203. 2018.– P. 40–48.
6. Alamdari S., et al., Preparation and Characterization of Zinc Oxide Nanoparticles Using Leaf Extract of Sambucus ebulus. Applied Science,– 10(10). 2020.– 3620 p.
7. Mohan Kumar K., et al., Synthesis and characterisation of flower shaped zinc oxide nanostructures and its antimicrobial activity. Spectrochim Acta A Mol Biomol Spectrosc,– 104. 2013.– P. 171–4.
8. Raoufi D. Synthesis and microstructural properties of ZnO nanoparticles prepared by precipitation method. Renewable Energy,– 50. 2013.– P. 932–937.
9. Vorobyova S. A., Lesnikovich A. I. and Mushinskii V. V. Interphase synthesis and characterization of zinc oxide. Materials Letters,– 58(6). 2004.– P. 863–866.
10. Shakti N. and Structural G. P.S, and Optical Properties of Sol-gel Prepared ZnO Thin Film. Applied Physics Research, 2010.– 2 p.

11. Wu Q.-H., ZnO nanostructures prepared using a vapour transport method. Journal of Experimental Nanoscience,– 10(3). 2015.– P. 161–166.
12. Segovia M., et al., Zinc Oxide Nanostructures by Solvothermal Synthesis. Molecular Crystals and Liquid Crystals,– 555(1). 2012. P. 40–50.
13. Chen S.-J., et al., Preparation and characterization of nanocrystalline zinc oxide by a novel solvothermal oxidation route. Journal of Crystal Growth,– 252(1). 2003.– P. 184–189.
14. Chen D., Jiao X. and Cheng G. Hydrothermal synthesis of zinc oxide powders with different morphologies. Solid State Communications,– 113(6). 1999.– P. 363–366.
15. Polsongkram D., et al. Effect of synthesis conditions on the growth of ZnO nanorods via hydrothermal method. Physica B: Condensed Matter,– 403(19). 2008.– P. 3713–3717.
16. Altemimi A., et al. Phytochemicals: Extraction, Isolation, and Identification of Bioactive Compounds from Plant Extracts. Plants (Basel), 2017.– 6(4).
17. Shaheena S., et al., Extraction of bioactive compounds from Psidium guajava and their application in dentistry. AMB Express,– 9(1). 2019.– 208 p.
18. Sampath Kumar N. S., et al. Extraction of bioactive compounds from Psidium guajava leaves and its utilization in preparation of jellies. AMB Express,– 11(1). 2021.– 36 p.
19. Biswas B., et al., Antimicrobial Activities of Leaf Extracts of Guava Psidium guajava L. on Two Gram-Negative and Gram-Positive Bacteria. International Journal of Microbiology, 2013.– 746165 p.
20. Magaña S. M., et al. Antibacterial activity of montmorillonites modified with silver. Journal of Molecular Catalysis A: Chemical,– 281(1). 2008.– P. 192–199.
21. Kannan K., et al., Structural studies of bio-mediated NiO nanoparticles for photocatalytic and antibacterial activities. Inorganic Chemistry Communications,– 113. 2020.– 107755 p.
22. Vinotha V., et al. Synthesis of ZnO nanoparticles using insulin-rich leaf extract: Anti-diabetic, antibiofilm and anti-oxidant properties. J Photochem Photobiol B,– 197. 2019.– 111541 p.